Food Chemistry: X 25 (2025) 102022

Contents lists available at ScienceDirect

Food Chemistry: X

journal homepage: www.sciencedirect.com/journal/food-chemistry-x

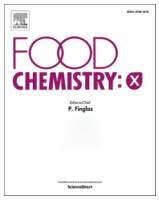

Assembly of oleosin during efficient extraction: Altering the sequence of defatting solvents

Yu Li [a], Yuqian Qiao [a], Yuxuan Zhu [a], Wangyang Shen [a], Weiping Jin [a,*], Dengfeng Peng [b], Qingrong Huang [c]

[a] School of Food Science and Engineering, Wuhan Polytechnic University, Wuhan, Hubei 430023, PR China
[b] Key Laboratory of Oilseeds Processing, Ministry of Agriculture, Oil Crops Research Institute, Chinese Academy of Agricultural Sciences, Wuhan 430062, PR China
[c] Department of Food Science, Rutgers University, 65 Dudley Road, New Brunswick, NJ 08901, USA

ARTICLE INFO

Keywords:
Oleosin
Protein assembly
Organic solvents
Extraction
Oil bodies

ABSTRACT

During the extraction of membrane proteins from oil bodies (OBs), organic solvents dissolve the lipid core and precipitate proteins through solvent stress. Here the effects of solvent type and defatting sequence on the composition and structure of membrane proteins were investigated *via* SDS-PAGE, FTIR, and SEM-EDS. High purity oleosin (86 %) was obtained by treatment first with a Floch solution and then with cold acetone and petroleum ether after twice washing OBs with urea. The 3D spatial structure of oleosin was predicted using AlphaFold 2, revealing that the secondary structure of oleosin was dominated by α-helices (>60 %). Oleosin consisted of two district types, with oleosin-H (16–17 kDa) being the part of the molecule with limited water solubility, while oleosin-L (13–14 kDa) constituted the non-soluble part. The results provided a technical means of efficient extraction of *Camellia* oleosins and selective separation of oleosin-L and oleosin-H.

1. Introduction

Oil bodies (OBs) are a subcellular structure in oilseed for lipid storage (De Chirico et al., 2020). Interestingly, OBs possess a natural emulsion structure, which is composed of a triacylglycerol core and an interfacial film co-stabilized by a monolayer of phospholipids and membrane proteins (Nikiforidis, 2019). Despite accounting for only 0.6–3.0 % of the total mass of OBs, these membrane proteins stabilize up to 70 % of the triacylglycerols (Pasaribu, Chen, Liao, Jiang, & Tzen, 2017), which are potential candidates for highly efficient surface-active substances (Plankensteiner, Hennebelle, Vincken, & Nikiforidis, 2024). Therefore, it is necessary to achieve a high yield extraction and understanding of conformational structure during the extraction.

The extraction of oil body membrane proteins (OBMPs) involves two steps. The first step is to obtain high purity OBs through aqueous extraction with the aid of enzymes (*e.g.*, carbohydrase, and proteases) or a buffer (*e.g.*, Tris-HCl and PBS) (Hao et al., 2022). Because the density of the lipid core in OBs is lower than that of water, OBs can easily cream and then be separated by centrifugation (Niu et al., 2024). The extracted pH is often adjusted to alkaline condition (pH 8.0–11.0), resulting in the removal of globulin and 2S albumin that also easily adsorbed on the surface of the OBs (Zhao, Chen, Chen, Kong, & Hua, 2016). To obtain purified OBs, urea and sodium dodecyl sulfonate (SDS) can be added to eliminate other impurities, including endogenous enzymes. The second step is removed the lipid core from OBs using organic solvents, such as cold acetone (Zhou, Chen, Hao, Du, & Liu, 2019), hexane (Lin, Liao, Yang, & Tzen, 2005), chloroform/methanol mixtures (D'Andréa et al., 2007; Vargo, Parthasarathy, & Hammer, 2012), diethylether (Nikiforidis et al., 2013), or a combination.

Organic solvents determine the purity, structure and property of membrane proteins. For example, the purity of oleosin extracted from *Arabidopsis thaliana* seed was only 16 % with a chloroform-methanol ratio of 5:4, whereas when the chloroform-methanol ratio elevated to 11:7, the extraction purity of oleosin increased to 78.7 % (D'Andréa et al., 2007). Plankensteiner et al. (2023) used methanol, hexane, and ethanol to extract the oleosin in sequence, and the extracted recovery

Abbreviations: OBs, oil bodies; OBMPs, oil body membrane proteins; A-PE, cold acetone-petroleum ether; C-M, chloroform-methanol; SDS-PAGE, sodium dodecyl sulfate polyacrylamide gel electrophoresis; FTIR, Fourier transform infrared spectroscopy; SEM-EDS, scanning electron microscope-energy dispersive spectrum; pLDDT, Per-residue Log Distance Deviation from the mean Trendline.

* Corresponding author.
E-mail address: jwpacademic@outlook.com (W. Jin).

https://doi.org/10.1016/j.fochx.2024.102022
Received 6 August 2024; Received in revised form 27 October 2024; Accepted 17 November 2024
Available online 20 November 2024

reached 94 ± 1.4 % with a purity of 87.1 ± 1.9 %. Besides, organic solvents also have a great impact on protein folding, assembled structure, and functional properties by modulating hydrophobic interactions and hydrogen bonds (Yu, Wang, Shao, Shi, & Zhu, 2016). Altering an organic solvent polarity can induce different protein conformations (Neubauer, Trossmann, Jacobi, Döbl, & Scheibel, 2021). For example, pre-cooled acetone treatment of laccase increased its enzyme activity by two times (Wu et al., 2019). Zhong et al. (2023) found that ethanol induced soybean lipophilic protein to assemble into nanoparticles that encapsulated resveratrol. When the ethanol content varied from 0 to 70 % (*v*/v), nanoparticles showed significant differences in the structure, size, and morphology. These findings are all attributed to the manipulation of protein-protein and protein-solvent interactions in organic solvents (Nandakumar, Ito, & Ueda, 2020).

This work focuses on *Camellia oleifera,* one of the world's four woody edible oil crops. Statistics in 2020 showed that China's annual production of *C. oleifera* reached 6.27 million tons, accounting for over 90 % of the world's production (Zhang et al., 2022). According to genome and transcriptome analyses, there are two types of OBMPs in OBs, oleosin and caleosin, that are directly related to lipid storage in *C. oleifera*, of which oleosin has the highest abundance and plays an essential role (Feng et al., 2017; Zhang et al., 2023). Here, organic solvents, including cold acetone, petroleum ether, and a chloroform-methanol mixture, were used for lipid removal and oleosin extraction in different combinations. The influence of solvent polarity on the extraction process, secondary structure, and assembled behavior of OBMPs were studied. This work offers an efficient solution to obtain *C. oleifera* oleosin for further applications.

2. Materials and methods

2.1. Materials

C. oleifera seeds were purchased from Quzhou farm, Zhejiang, China. Chemical reagents, such as urea, NaOH, NaCl, acetone, petroleum ether, chloroform, and methanol were analytical grade, and were supplied from Sinopharm Group Chemical Reagent Co., LTD (Shanghai, China). Deionized water (DI) was obtained using a Milli-Q Water system (Merck Millipore, Billerica, MA, USA) with a resistivity of 18.2 MΩ·cm.

2.2. Extraction and purification of oil bodies

The OBs were extracted using an aqueous extraction method, as shows in Fig. 1 (Niu et al., 2024). First, the *C. oleifera* seeds and deionized water were homogenized at a ratio of 1:4–1:99 for 3 min using a blender (M-WBL2521H, Midea, Guangzhou, China), the pH of the mixture was adjusted to 9.0–11 by adding NaOH, and the mixture was stirred for 30 min. The slurries were filtered with 200 mesh gauze, centrifuged at 6000 ×*g* for 30 min, and the cream layer was obtained as the crude OBs. Next, the corresponding pH solution was added into the crude OBs at a ratio of 1:5, stirred for 10 min, and centrifuged at 10,000 ×*g* for 10 min. The bottom phase was discarded, and the cream phase was washed using urea (0.8–6.4 M) with 1–3 times. During each washing cycle, the duration of mixing was 10 min, and dispersions were centrifuged at 10,000 ×*g* for 10 min. Finally, deionized water was added at a 1:5 ratio to remove residual urea, and the purified OBs were obtained as the cream layer after centrifugation at 10,000 ×*g* for 10 min. The yield of OBs extracted with different parameters was calculated according to the following equation:

$$OB\ yield\ (wt\%) = \frac{\text{g of purified OBs}}{\text{g of seeds weighed as raw materials}} \times 100$$

2.3. Extraction of oil body membrane proteins

The organic solvents used to remove the lipid core of OBs comprised four types: cold acetone-petroleum ether, chloroform-methanol (2:1), cold acetone-petroleum ether/chloroform-methanol, and chloroform-methanol/cold acetone-petroleum ether. The process is shown in Fig. 1. The specific steps were as follows: 1 mL cold acetone was added to 0.5 mL of OBs cream, vortexed for 3 min, and centrifuged for 1 min at 10,000 ×*g*. The organic phase was discarded and 1 mL of petroleum ether was added to the sediment, vortexed for 3 min, and then centrifuged at 10,000 ×*g* for 1 min. For other samples, 1 mL of chloroform-methanol (2:1) was used instead of cold acetone or petroleum ether, and the process then proceeded with the same steps. Finally, the precipitate part was dried naturally under a hood, and marked as oil body membrane proteins (OBMPs).

2.4. Measurement of protein content

The protein content was determined using an elemental analyzer (Elementar *V*ario EL Cube, Germany) (Dong, Xiao, Xian, & Wu, 2018). The OBMP samples (2.0–5.0 mg) were weighed in aluminum boxes, pressed and sealed, and placed in the sample tank of the element analyzer for determination. The test time was 90 s. After determining the content of N element, the data was multiplied by 6.25 to get the protein content.

2.5. Sodium dodecyl sulfate polyacrylamide gel electrophoresis

The OBs cream (20 μL) or an OBMP solution (1.0–2.0 mg dissolved in 0.1 M SDS, 20 μL) was diluted twice, and then 10 μL of loading buffer was added. The mixtures were boiled for 10 min, centrifuged at 600 ×*g* for 1 min, and 10 μL was used to load gel Marker (10–180 kD, Beyotime Biotechnology). The operating voltage was set at 60 V, the running time in the 5 % stacking gel was 30 min, and the electrophoresis time in the 12 % resolving gel was 80 min. After electrophoresis, the gels were dyed with Coomassie Brilliant Blue G250 for 30 min and then decolored. Finally, bands in the gels were analyzed using a ChemiDoc MP imaging system (Bio-Rad, Laboratories, CA, USA) (Chen et al., 2023).

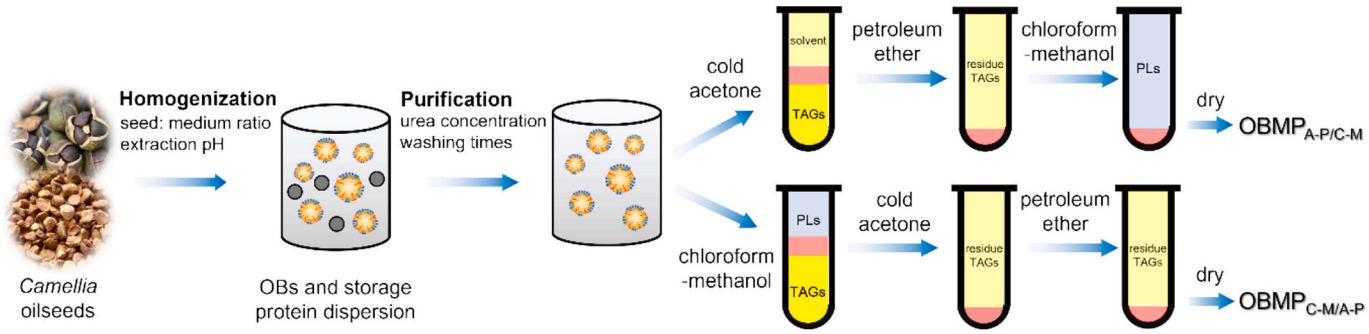

Fig. 1. General extraction process for OBMPs from *Camellia* seeds. PLs and TAGs represent phospholipids and triglycerides, respectively.

2.6. Fourier transform infrared spectroscopy

The FTIR spectra of the OBMPs were measured using an infrared spectroscope (Frontier, PerkinElemer Inc., Waltham, MA, USA). Powders of OBMPs and KBr were thoroughly mixed at a 1:100 ratio and laminated. The parameters of the transmission mode were set as follows: wavenumber of 4000–400 cm^{-1}, scanning time of 32, and resolution of 4 cm^{-1}. The background signal of KBr was deducted before scanning (Jin et al., 2023). A baseline correction and second-order derivatives of the amide band I were applied. The content of the secondary structure of the OBMPs was determined by Gaussian split-peak fitting using Origin software.

2.7. Scanning electron microscope-energy dispersive spectrum

OBMPs were adhered to a sample platform and sprayed with gold for 45 s using a sputter coater at 10 mA (Khalesi & FitzGerald, 2021). Subsequently, the microstructure of the samples was observed using a scanning electron microscope (SEM 300, ZEISS, Germany) for topography and energy spectrum mapping, with an accelerating voltage of 3 k*V* for topography and 15 kV for energy spectrum mapping, and with an SE2 secondary electron detector as the detector.

2.8. Solubility of proteins

OBMPs (1.0 mg) were dissolved in 1.0 mL deionized water or buffer (0.005–0.015 M NaCl, 0.0025–0.1 M SDS, and 0.2–0.8 M urea) (Peng et al., 2023). The centrifuge tube was placed under ultrasonication for 10 min, and then vortexed for 30 min. The dissolving step was repeated three times. After centrifugation at 10,000 ×*g* for 3 min, the supernatant underwent bicinchoninic acid analysis to determine the soluble protein fraction using a standard curve of $y = 0.78\times–0.08$ ($R^2 = 0.99$).

2.9. Three-dimensional modeling of oleosin using AlphaFold 2

The amino acid sequences of several oleosins, using Ole I, Ole III, and Ole V as examples, were downloaded from the NCBI database (https://www.ncbi.nlm.nih.gov/) in FASTA format with GenBank numbers ABF 57559.1, ABF 57563.1, and ABF 57562.1. The 3D models of the oleosins were constructed using AlphaFold 2 software (Jumper et al., 2021). The Per-residue Log Distance Deviation from the mean Trendline (pLDDT) was used to measure the reliability of each amino acid residue in a given protein model, which was calculated by comparing the distance deviation of a structural model with the mean trendline of a known structure. Then, SAVES v6.0 (https://servicesn.mbi.ucla.edu/SAVES/) was used to evaluate the model.

2.10. Statistic analysis

In all tests, measurements were repeated in triplicate. Data were expressed as the mean value ± standard deviation. Statistical analysis and plotting were performed using SPSS 23 (IBM Corporation, Armonk, NY, USA) and Origin 2021 (Origin Lab Corporation, Northampton, MA, USA). The univariate analysis of variance (ANOVA) was used to calculate the significant difference of the results, with a significance level of $P < 0.05$.

3. Results and discussion

3.1. Extraction and purification of OBs

The first step for obtaining OBMPs involves extracting OBs with a high yield. Fig. 2A shows that the yield of OBs increased first and then decreased with increasing the seed-medium ratio. When the seed-medium ratio was 1:4, the increased viscosity of the slurry during the grinding process hindered cell disruption and release of the OBs, leading to buoyancy resistance in the centrifugation separation (De Chirico, di Bari, Foster, & Gray, 2018). Conversely, a high seed-medium ratio (1:49 and 1:99) promoted cell rupture during grinding and reduced the damage to the OBs. In fact, centrifugation separation of a large volume of slurries was time-consuming and costly, and the cream layer was too loose to collect. Therefore, the optimal condition for recovering OBs was a seed-medium ratio of 1:9 (yield of 13.83 %). The proteins in the OBs were analyzed by SDS-PAGE, and there was no obvious difference between seed-medium ratios based on the intensity of the bands, among which the darkest band was oleosins (13–17 kDa).

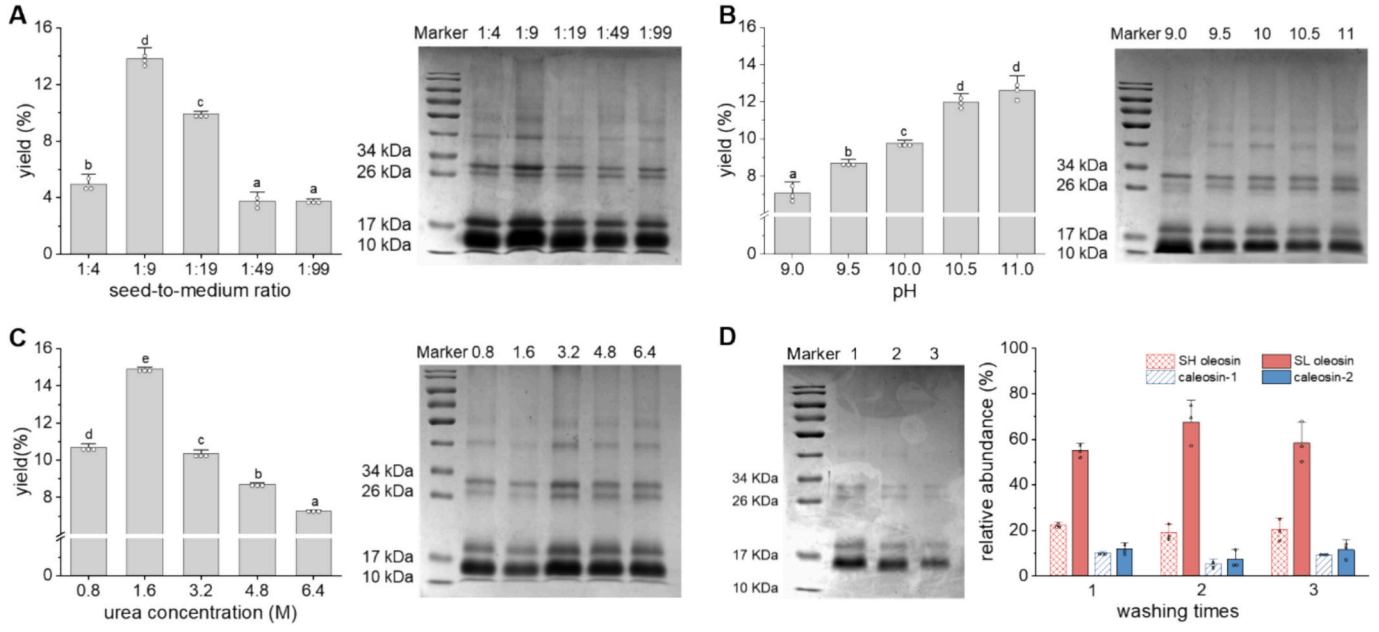

Fig. 2. Effects of extraction and purification parameters of OBs from *Camellia* seeds on the yield and SDS-PAGE images of OBMPs, (A) seed-medium ratio, (B) pH, and (C) urea concentration. (D) Effect of number of washes on the SDS-PAGE bands and relative abundance of oleosin and caleosins, respectively. Data are reported as mean ± s.d. of three independent replications. Lowercase in the figure represent significant differences between data ($p < 0.05$).

Because the isoelectric point of the OBs was generally lower than 7.0, droplets carried sufficient negative charges under an alkaline pH to prevent aggregation and maintain the stability of the OBs during the extraction (Hao et al., 2022). The effect of pH on the yield of OBs is shown in Fig. 2B. As pH increased, the yield of OBs also increased, but there was no significant difference between yields at pH 10.5 and 11 ($p < 0.05$). The electrophoretic bands obtained through alkaline extraction were similar. Bands of oleosin remained broad and dark, indicating that alkaline conditions helped remove the extrinsic proteins, such as albumin, globulin, and enzymes, that easily adsorbed on the surface of OBs (Zhao et al., 2016), but had no negative effect on oleosins; therefore, pH 10.5 was selected to for further purification of OBs.

Urea is a rigorous washing agent that can effectively remove exogenous seed proteins, maintain the stability of OBs, and extract the integral oleosin (De Chirico et al., 2018). The highest yield of OBs (14.89 ± 0.07 %) was achieved with a urea concentration of 1.6 M after a single wash (Fig. 2C). However, increasing the urea concentration beyond 1.6 M led to a significant decrease in the yield of OBs ($P < 0.05$). SDS-PAGE results showed that bands from different urea treatments exhibited similar patterns, suggesting that urea had no visible influence on the composition and integrity of interfacial properties. After repeated washing with 1.6 M urea two to three times, electrophoretic bands above 34 kDa disappeared, but oleosin (13–17 kDa) and caleosin (27–30 kDa) bands were still clear. According to the oleosin family genes identified in *C. oleifera* (Zhang et al., 2023), two distinct oleosin linkages were found: (*i*) low molecular-weight (SL) seed oleosin, in which the protein length is 127–141 amino acids with a molecular weight of 13.4–14.8 kDa; and (*ii*) high molecular-weight (SH) oleosin, in which the protein length is 148–157 amino acids with a molecular weight of 15.9–16.8 kDa. As shown in Fig. 2D, electrophoretic bands were consistent with the gene analysis. Moreover, the intensity of the bands was used to calculate the relative abundances of oleosin and caleosin using image analysis software. There was no significant difference in the relative abundance of oleosin and caleosin during urea washing process. After washing twice, the relative abundance of oleosins was 86 % (19.55 % for oleosin-L and 66.45 % for oleosin-H), while caleosin accounted for 14 %. Thus, the optimal purification parameters for recovering intact oleosins was a urea concentration of 1.6 M and two washes.

3.2. Effect of organic solvents on the morphology and structure of OBMPs

Because OBMPs are located at the oil–water interface, the extract needs to be defatted with added organic solvents. Commonly used organic solvents for de-oiling or defatting processes includes cold acetone, petroleum ether, and chloroform-methanol mixtures (Folch solution). Different organic solvents have various efficiencies in oil extraction and composition of residual proteins (Gao, Liu, Jin, & Wang, 2019). Microstructural images and surface element analyses of OBMPs obtained by adding organic solvents in different sequences were investigated using SEM-EDS (**Fig. 3A** and **B**). In the 1st treatment, cold acetone and petroleum ether (A-PE) were initially added, resulting in the retention of phospholipids that stabilized the interface, while neutral lipids in the triacylglycerols core were removed *in situ*, forming a porous structure. Subsequently, chloroform-methanol (C-M) mixtures were used to remove phospholipids on the surface of the pore, resulting in a lotus seedpod shape. In the 2nd treatment, the addition of C-M mixture destroyed the phospholipid layer and caused the destabilization of OBs, resulting in droplet coalescence. The neutral lipids were removed more effectively after continuously adding A-PE, and OBMPs aggregated together. The results indirectly indicated that phospholipids play an important role in OBs stability. The elements and components of OBMPs in the SEM micro-view were analyzed through an EDS mapping scan (**Fig. 3C** and **D**). The elements N represents the unique composition of protein, while P represents phospholipid. The N:P ratio at the $OBMP_{A\text{-}PE/C\text{-}M}$ surface was lower than that of $OBMP_{C\text{-}M/A\text{-}PE}$. Additionally, the C:N ratio in $OBMP_{A\text{-}PE/C\text{-}M}$ was 4.10, but it decreased to 1.85 in $OBMP_{C\text{-}M/A\text{-}PE}$, also suggesting that $OBMP_{C\text{-}M/A\text{-}PE}$ was conducive to the complete removal of phospholipids and neutral lipids.

The removal of lipids from OBs was incompletely when using cold acetone/ petroleum ether and a chloroform-methanol mixture alone, resulting in a low protein content (Fig. 4A). According to results of our previous studies (Jin et al., 2023), the combinations of different organic solvents in sequence had the following effect on the protein content of OBMPs: $OBMP_{A\text{-}PE} < OBMP_{C\text{-}M} < OBMP_{A\text{-}PE/C\text{-}M} < OBMP_{C\text{-}M/C\text{-}M/C\text{-}M} < OBMP_{C\text{-}M/A\text{-}PE} \sim OBMP_{A\text{-}PE/A\text{-}PE/A\text{-}PE}$. The first stress of organic solvents mainly affected the microstructure of OBMPs, while the final stress determined the protein content and residual lipids in OBMPs. If the final

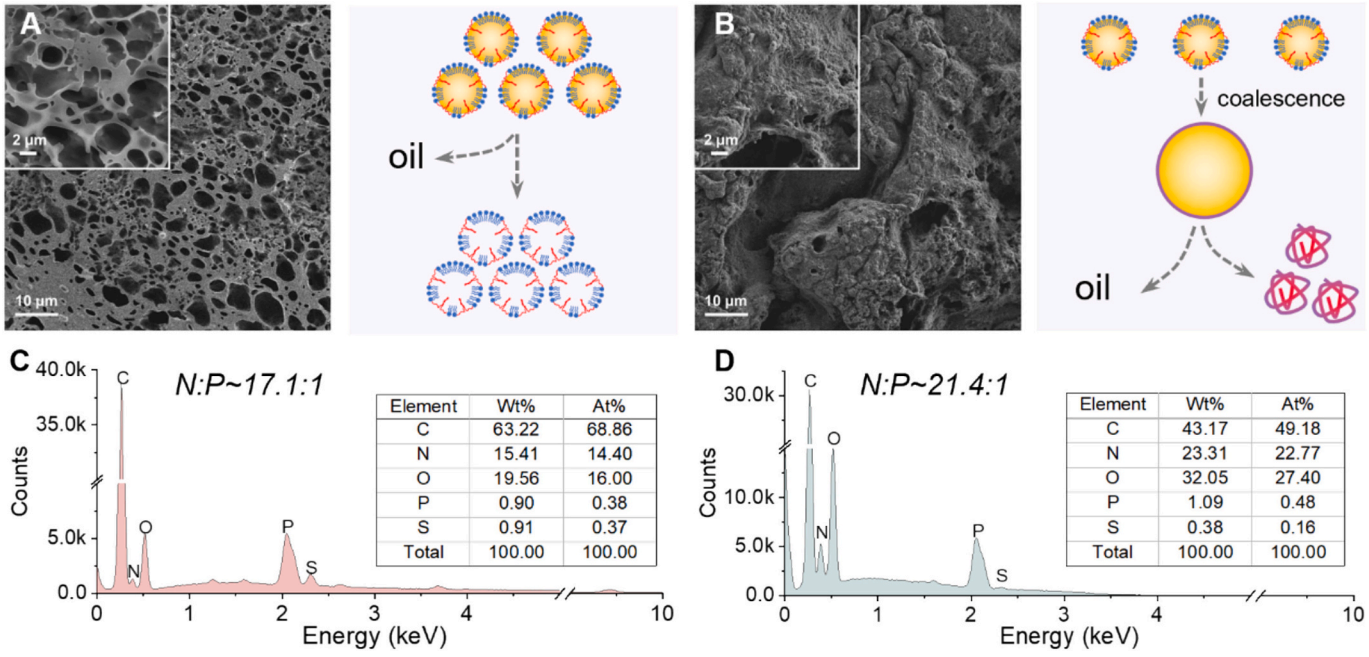

Fig. 3. Effect of organic solvents on the microstructure of OBMPs. (A, B) Representative SEM images of $OBMP_{A\text{-}PE/C\text{-}M}$ and $OBMP_{C\text{-}M/A\text{-}PE}$, and (C, D) corresponding EDS analysis of the nitrogen and phosphorous distribution on the surface of $OBMP_{A\text{-}PE/C\text{-}M}$ and $OBMP_{C\text{-}M/A\text{-}PE}$.

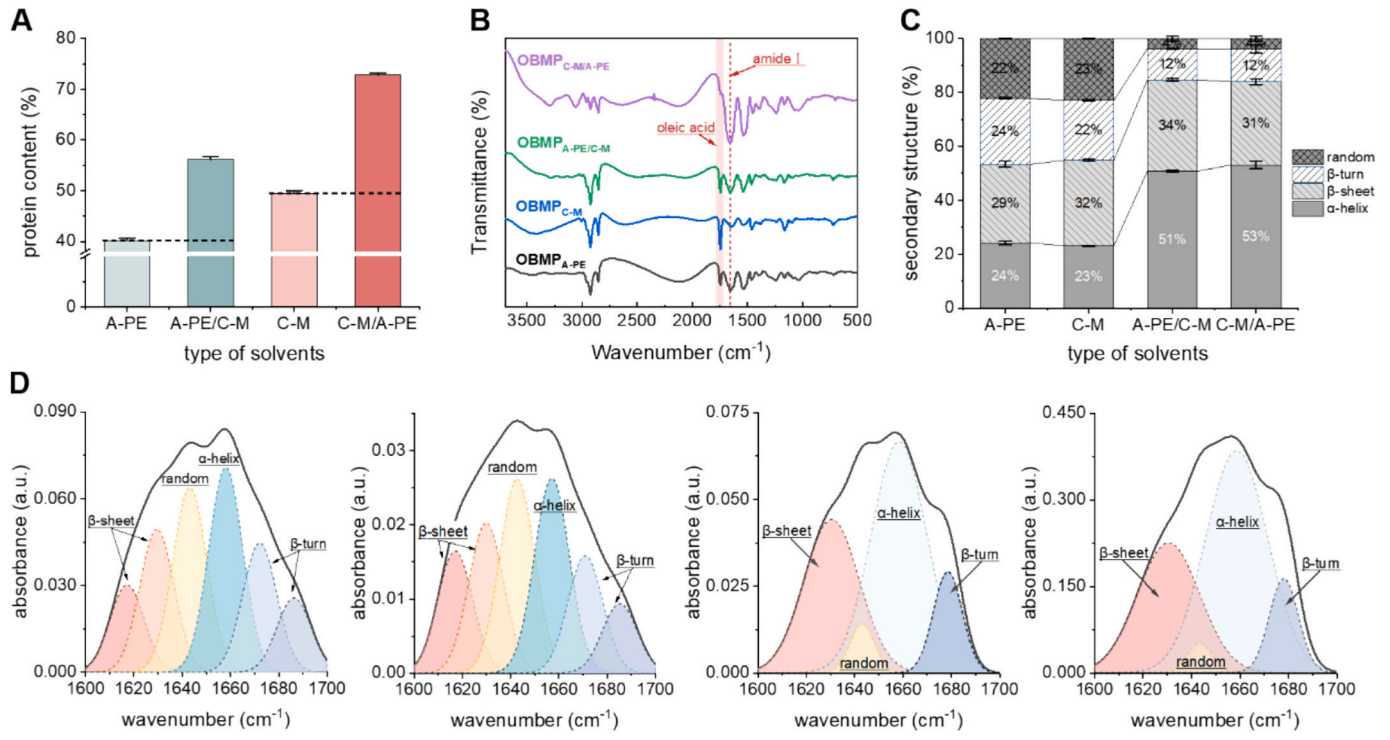

Fig. 4. Effect of organic solvents on the purity and secondary structure of OBMPs. (A) protein content, (B) FTIR spectrum, (C) percentage of secondary structures, and (D) peak fitting of amide band I. Data in A and C are reported as mean ± s.d. of three independent replications.

solvents were A-PE, it benefitted the lipid removal and produced high-purity OBMPs. The protein content of OBMPs washed with A-PE three times was similar to that of OBMPs washed with C-M and A-PE, indicating that the combination of C-M and A-PE solvents improved the extraction efficiency of OBMPs and reduced the extra use of A-PE solvents. The effects of organic solvents on the secondary structure of OBMPs was further analyzed by infrared spectroscopy (Fig. 4B). The spectra of $OBMP_{A\text{-}PE}$, $OBMP_{C\text{-}M}$, and $OBMP_{A\text{-}PE/C\text{-}M}$ had an obvious absorption peak at 1710 cm^{-1}, which was ascribed to the characteristic peak of oleic acid (Yang, Peng, Wen, & Li, 2010). Oleic acid constitutes nearly 80 % of the fatty acid in camellia oil (Zhang et al., 2022); therefore, the results indicated the presence of lipid residue in the samples. The absorption of this peak in $OBMP_{C\text{-}M/A\text{-}PE}$ was very weak, so it had a high protein content. To quantitatively analyze the secondary structure of OBMPs, a Gaussian deconvolution and the second derivative analysis were performed on the amide band I (1600–1700 cm^{-1}), identifying six points with the second derivative equal to zero (**Fig. 4C** and **D**). Peaks observed at 1618 cm^{-1} and 1630 cm^{-1} were attributed to β-sheets, while those at 1670 cm^{-1} and 1686 cm^{-1} were attributed to β-turns. Peaks at 1640 cm^{-1} and 1660 cm^{-1} were ascribed to a random coil and α-helix, respectively. The secondary structure of $OBMP_{A\text{-}PE}$ and $OBMP_{C\text{-}M}$ exhibited similar characteristics, with 23–24 % α-helix, 29–32 % β-sheet, 22–24 % β-turn, and ~ 22 % random coil structure. When OBMPs were treated with two rounds of organic solvents, the proportion of α-helix structures increased to 51–53 %, while that of β-turns and random coils decreased significantly. This suggested that the removal of neutral lipids and phospholipids significantly affected the secondary structure of the protein, but had no obvious relationship with the sequence of solvent treatments.

3.3. Effect of organic solvents on assembly behavior of OBMPs and potential mechanism

The types and sequence of organic solvents used for lipid removal altered the microstructure of OBMPs by changing the destabilization mechanism and process of OBs, but had no significant influence on the secondary structure of the proteins. Therefore, it was hypothesized that a key factor to determine the microstructure of OBMPs was the difference in the protein assembly and aggregation behavior (Sun et al., 2021). The driving force of the protein aggregation could be deduced by using disrupting agents during the dissolution process of OBMPs. For example, sodium chloride (NaCl) is used to disrupt electrostatic interactions by increasing the charge on the surface of proteins. Urea interferes hydrogen bonds between protein molecules, and SDS disrupts hydrophobic interactions (Peng et al., 2023). As depicted in Fig. 5A, oleosins are highly hydrophobic and have extremely low water-solubility due to the large hydrophobic central region in oleosin, which accounts for more than 50 % of its amino acid sequence. The solubilities of $OBMP_{A\text{-}PE/C\text{-}M}$ and $OBMP_{C\text{-}M/A\text{-}PE}$ were only 4.6 % and 12.7 %, respectively. After adding 0.01 M NaCl and 0.4 M urea, the water-solubility of $OBMP_{A\text{-}PE/C\text{-}M}$ increased to 12.9 % and 14.5 %, respectively. NaCl and urea had no significant effect on the water-solubility of $OBMP_{C\text{-}M/A\text{-}PE}$. The limited increase in water-solubility of $OBMP_{A\text{-}PE/C\text{-}M}$ could be attributed to the electrostatic interaction and hydrogen bonding between residual phospholipids and oleosins (Deleu et al., 2010). However, when 0.025 M and 0.1 M SDS was added, the solubility of $OBMP_{A\text{-}PE/C\text{-}M}$ and $OBMP_{C\text{-}M/A\text{-}PE}$ greatly increased to 62.1 % and 58.9 %, respectively, indicating that the hydrophobic interactions were the main driving force of OBMP assembly and aggregation.

After dissolving OBMPs extracted with different organic solvents in SDS, $OBMP_{C\text{-}M/C\text{-}M}$, $OBMP_{A\text{-}PE/A\text{-}PE}$, $OBMP_{A\text{-}PE/C\text{-}M}$, and $OBMP_{C\text{-}M/A\text{-}PE}$ both had intense bands at 13–14 kDa (oleosin-L) and 26–30 kDa (caleosin). The results showed that the three types of OBMPs could be successfully extracted using organic solvent. The main difference was observed in the band at 16–17 kDa (oleosin-H), which indicated that repeated use of C-M solution could result in the loss of oleosin-H. Next, the water-insoluble part of $OBMP_{C\text{-}M/A\text{-}PE}$ and $OBMP_{A\text{-}PE/C\text{-}M}$ was collected and redissolved in 0.1 M SDS for further analysis. Comparing the electrophoretic bands of insoluble and total OBMPs, the oleosin-H band disappeared in $OBMP_{C\text{-}M/A\text{-}PE}$ and it became shallow in $OBMP_{A\text{-}PE/C\text{-}M}$. The results indicated that oleosin-H and caleosin more easily solubilized, while the aggregates formed by oleosin-L were difficult to

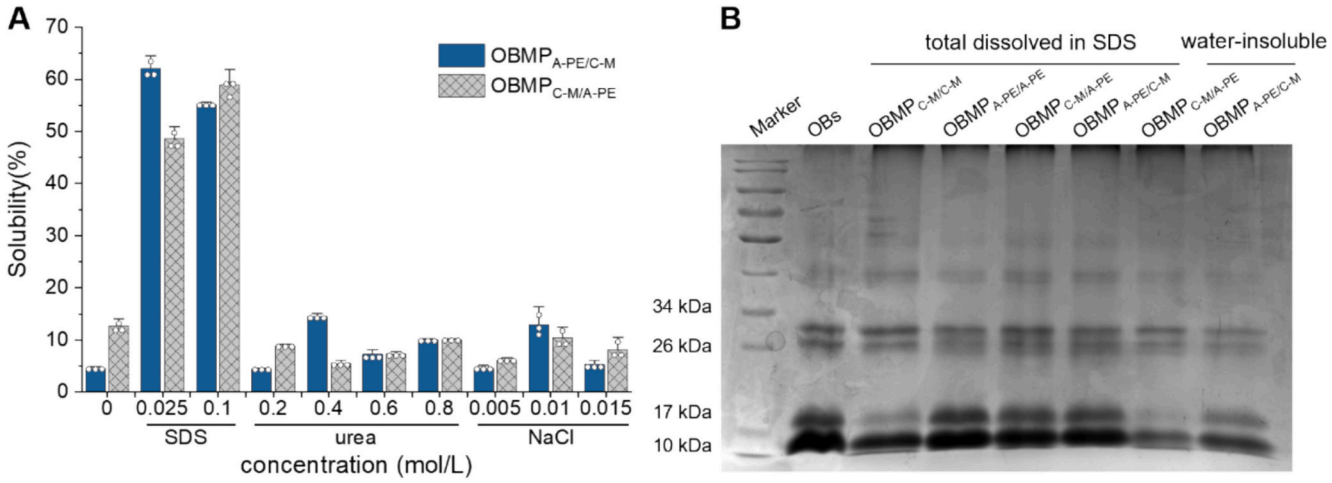

Fig. 5. Speculation of the driving forces of OBMPs assemblies induced by organic solvent shock during lipid removal. (A) Solubilities of $OBMP_{A\text{-}PE/C\text{-}M}$ and $OBMP_{C\text{-}M/A\text{-}PE}$ in water, SDS, urea, and NaCl, (B) SDS-PAGE image of OBs, totally soluble parts of $OBMP_{C\text{-}M/C\text{-}M}$, $OBMP_{A\text{-}PE/A\text{-}PE}$, $OBMP_{C\text{-}M/A\text{-}PE}$, and $OBMP_{A\text{-}PE/C\text{-}M}$ in 0.1 M SDS, and water-insoluble parts of $OBMP_{C\text{-}M/A\text{-}PE}$, and $OBMP_{A\text{-}PE/C\text{-}M}$.

dissolve in water. These results indicated that oleosin-H was more hydrophilic than oleosin-L, and had a larger solubility in the aqueous phase or polar solvent C-M. Finally, the differences in water solubility of the aggregates formed by oleosin-L and oleosin-H were analyzed from the perspective of the amino acid sequence and 3D structure.

3.4. Prediction of oleosin structure

In the NCBI database, there are five identified *C. oleifera* oleosins, oleosin (Q1G352, 141AA), Ole III (Q1G349, 140AA), Ole I*V* (Q1G351, 154AA), Ole I (Q1G353, 148AA), and Ole V (Q1G350, 157AA). Ole I, Ole III, and Ole V were selected for analysis of their amino acid sequences, and the results showed that they differed in the N-terminal (Fig. 6A, and **Table S1**). The central hydrophobic regions of the three oleosin were conserved and similar. The predicted secondary structure of the C-terminal was dominated by alpha-amphipathic regions, with some beta-amphipathic regions exhibiting crossover. The amphipathic and flexible characteristics of the C-terminal stabilized the oil–water interface, increased the steric resistance between OBs droplets, and promoted their stability. For a protein with a homologous sequence that is difficult to match with existing structures, such as oleosin, AlphaFold 2 is a candidate for predicting the spatial structure (Luo et al., 2024). First, the reliability of the protein structure was assessed by pLDDT (**Fig. S1**) by comparing the distance deviation of a structural model with the mean trendline of a known structure. The pLDDT commonly ranges from 0 to 100, and a higher score indicates a higher quality and reliability of the protein structure (Zhou et al., 2024). The average pLDDTs of the three oleosins were all greater than 70, indicating that the protein model was sufficient. Next, the oleosin models that were built were then evaluated *via* SAVES v6.0 (https://servicesn.mbi.ucla.edu/SAVES/). From a Ramachandran plot (**Fig. S1**), the residues in the most favored regions [A, B, L] of Ole I, Ole III, and Ole V were 104 (83.9 % of the total sequence), 112 (94.1 % of the total sequence), and 110 (85.3 % of the total sequence), respectively. The residues in additional allowed regions [a, b, l, p] of Ole I, Ole III, and Ole V were 15 (12.1 % of the total sequence), 7 (5.9 % of the total sequence), and 10 (7.8 % of the total sequence), respectively. Therefore, the summary of the most favored and additional allowed regions of Ole I, Ole III, and Ole V were 99.2 %, 100 %, and 99.2 %, respectively. This suggested that the prediction of the protein conformation of the three oleosins was reasonable. The obtained 3D models of the oleosins (Fig. 6B) were basically consistent with the descriptions in previous literature (Huang & Huang, 2017). The central hydrophobic region of oleosins was arranged by two inverted α-helices to form a hairpin structure. The C- terminal was a flexible region dominated by an α-helix, while the N-terminal exhibited significantly differences. Ole I had a flexible random coil at the N-terminal, while Ole III had a short random coil with a short α-helix segment. The N-terminal of Ole V contained both an α-helix and a longer random coil. These structural variations determined the assembly behavior and solubility of proteins after organic solvent stress. To be specific, the molecular weight of Ole V is approximately 17.3 kDa and it belongs to oleosin-H, which possesses more hydrophilic regions in the N-terminal and a looser secondary structure, making it more prone to dissolution in water, or easier dissociation from the oil–water interface during extraction with polar solvent. The predicted structure was in agreement with the experimental results.

4. Conclusion

A high purity of OBs was extracted under an alkaline pH (> 10.5) and washed with 1.6 M urea twice. The type and extraction sequence of organic solvents were used to determine the protein content and microstructure of the OBMPs. The first stress of the solvents primarily affected the microstructure of the OBMPs, and the second stress of the solvents determined the protein content and residues of lipids. If the second solvents were cold acetone and petroleum ether, it benefitted the lipid removal and produced high-purity OBMPs. Regardless of the solvent sequence, the secondary structure of OBMPs were chiefly α-helices. The main driving force behind oleosin assembly was hydrophobic interactions. Oleosin-L and oleosin-H could be separated based on their water solubility. Understanding of oleosin assembling behavior would benefit in controlling the assembly and inspire us to design a new Pickering particle for stabilizing emulsions based on assemblies of oleosin-H.

CRediT authorship contribution statement

Yu Li: Writing – original draft, Formal analysis, Data curation. **Yuqian Qiao:** Formal analysis, Data curation. **Yuxuan Zhu:** Methodology, Data curation. **Wangyang Shen:** Project administration, Methodology, Formal analysis. **Weiping Jin:** Writing – original draft, Supervision, Funding acquisition, Conceptualization. **Dengfeng Peng:** Writing – review & editing, Methodology, Formal analysis. **Qingrong Huang:** Writing – review & editing, Conceptualization.

Declaration of competing interest

We declare that we have no financial and personal relationships with

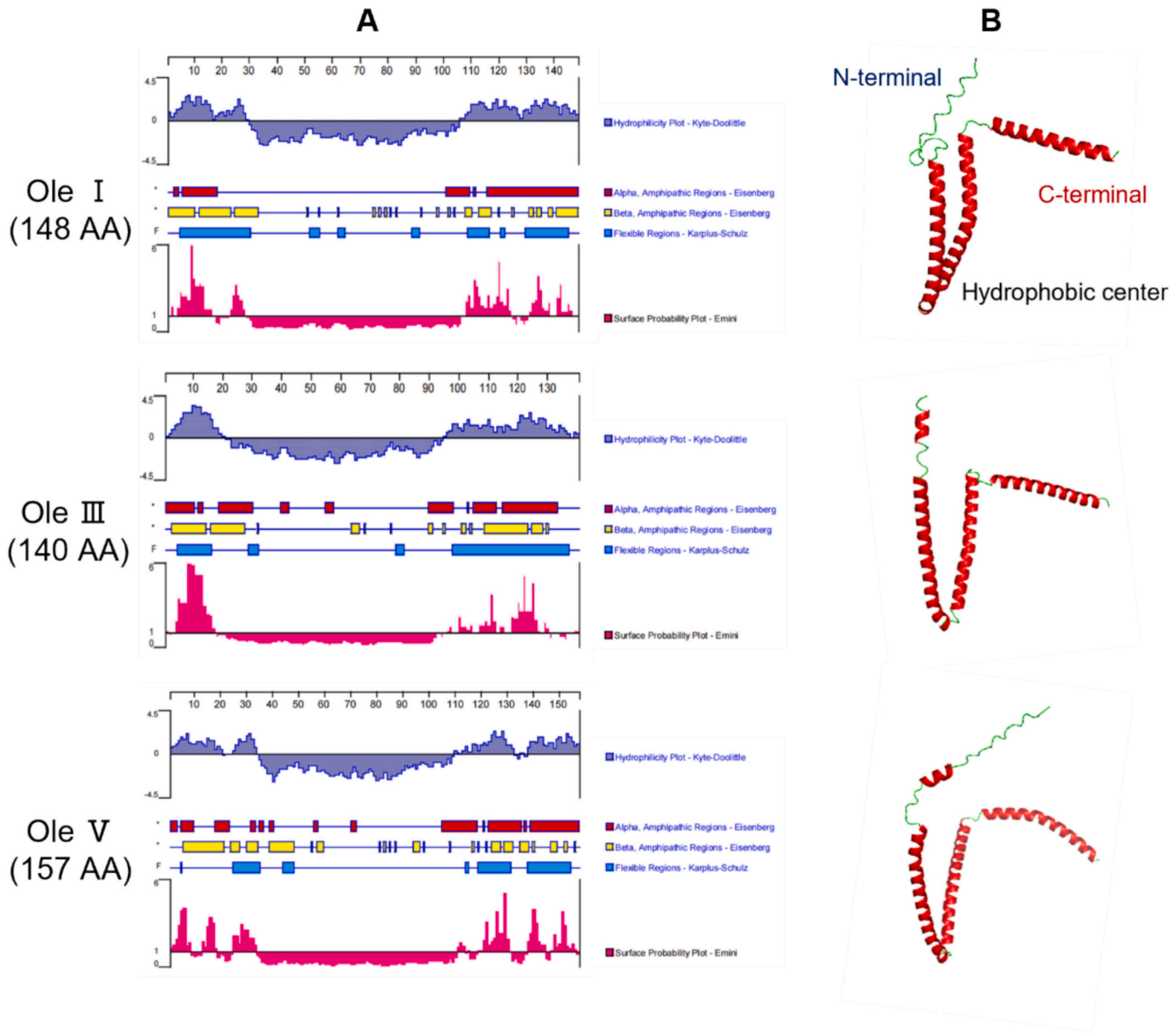

Fig. 6. Prediction of the hydrophobicity and amphipathic region, flexible region, surface probability, and spatial structure of Ole I, Ole III, and Ole V. (A) Amnio acid sequence properties analyzed by DNAStar, and (B) 3D models of ternary structures built by AlphaFold 2 modeling.

other people or organizations that can inappropriately influence our work.

There is no professional or other personal interest of any service and/or company that could be construed as influencing the position presented in the manuscript.

No conflict of interest exits in the submission of this manuscript, and manuscript is approved by all authors for publication. All the authors listed have approved the manuscript that is enclosed.

Acknowledgement

This research was funded by the National Natural Science Foundation of China (No. 32072152).

Appendix A. Supplementary data

Supplementary data to this article can be found online at https://doi.org/10.1016/j.fochx.2024.102022.

Data availability

Data will be made available on request.

References

Chen, C., Pan, Y., Niu, Y., Peng, D., Huang, W., Shen, W., & Huang, Q. (2023). Modulating interfacial structure and lipid digestion of natural Camellia oil body by roasting and boiling processes. *Food Chemistry, 402*, Article 134198. https://doi.org/10.1016/j.foodchem.2022.134198

D'Andréa, S., Jolivet, P., Boulard, C., Larré, C., Froissard, M., & Chardot, T. (2007). Selective one-step extraction of *Arabidopsis thaliana* seed oleosins using organic solvents. *Journal of Agricultural and Food Chemistry, 55*(24), 10008–10015. https://doi.org/10.1021/jf0717079

De Chirico, S., di Bari, V., Foster, T., & Gray, D. (2018). Enhancing the recovery of oilseed rape seed oil bodies (oleosomes) using bicarbonate-based soaking and grinding media. *Food Chemistry, 241*, 419–426. https://doi.org/10.1016/j.foodchem.2017.09.008

De Chirico, S., di Bari, V., Romero Guzmán, M. J., Nikiforidis, C. V., Foster, T., & Gray, D. (2020). Assessment of rapeseed oil body (oleosome) lipolytic activity as an effective predictor of emulsion purity and stability. *Food Chemistry, 316*, Article 126355. https://doi.org/10.1016/j.foodchem.2020.126355

Deleu, M., Vaca-Medina, G., Fabre, J.-F., Roïz, J., Valentin, R., & Mouloungui, Z. (2010). Interfacial properties of oleosins and phospholipids from rapeseed for the stability of oil bodies in aqueous medium. *Colloids and Surfaces B: Biointerfaces, 80*(2), 125–132. https://doi.org/10.1016/j.colsurfb.2010.05.036

Dong, H., Xiao, K., Xian, Y., & Wu, Y. (2018). Authenticity determination of honeys with non-extractable proteins by means of elemental analyzer (EA) and liquid chromatography (LC) coupled to isotope ratio mass spectroscopy (IRMS). *Food Chemistry, 240*, 717–724. https://doi.org/10.1016/j.foodchem.2017.08.008

Feng, J.-L., Yang, Z.-J., Bai, W.-W., Chen, S.-P., Xu, W.-Q., El-Kassaby, Y. A., & Chen, H. (2017). Transcriptome comparative analysis of two Camellia species reveals lipid metabolism during mature seed natural drying. *Trees, 31*(6), 1827–1848. https://doi.org/10.1007/s00468-017-1588-5

Gao, P., Liu, R., Jin, Q., & Wang, X. (2019). Comparison of solvents for extraction of walnut oils: Lipid yield, lipid compositions, minor-component content, and antioxidant capacity. *LWT-Food Science and Technology, 110*, 346–352. https://doi.org/10.1016/j.lwt.2019.04.100

Hao, J., Li, X., Wang, Q., Lv, W., Zhang, W., & Xu, D. (2022). Recent developments and prospects in the extraction, composition, stability, food applications, and in vitro digestion of plant oil bodies. *Journal of the American Oil Chemists' Society, 99*(8), 635–653. https://doi.org/10.1002/aocs.12618

Huang, C.-Y., & Huang, A. H. C. (2017). Unique motifs and length of hairpin in oleosin target the cytosolic side of endoplasmic reticulum and budding lipid droplet. *Plant Physiology, 174*(4), 2248–2260. https://doi.org/10.1104/pp.17.00366

Jin, W., Yang, X., Shang, W., Wu, Y., Guo, C., Huang, W., & Peng, D. (2023). Assembled structure and interfacial properties of oleosome-associated proteins from Camellia oleifera as natural surface-active agents. *LWT-Food Science and Technology, 173*, Article 114318. https://doi.org/10.1016/j.lwt.2022.114318

Jumper, J., Evans, R., Pritzel, A., Green, T., Figurnov, M., Ronneberger, O., & Hassabis, D. (2021). Highly accurate protein structure prediction with AlphaFold. *Nature, 596*(7873), 583–589. https://doi.org/10.1038/s41586-021-03819-2

Khalesi, M., & FitzGerald, R. J. (2021). Physicochemical properties and water interactions of milk protein concentrate with two different levels of undenatured whey protein. *Colloids and Surfaces A: Physicochemical and Engineering Aspects, 629*, Article 127516. https://doi.org/10.1016/j.colsurfa.2021.127516

Lin, L.-J., Liao, P.-C., Yang, H.-H., & Tzen, J. T. C. (2005). Determination and analyses of the N-termini of oil-body proteins, steroleosin, caleosin and oleosin. *Plant Physiology and Biochemistry, 43*(8), 770–776. https://doi.org/10.1016/j.plaphy.2005.07.008

Luo, X., Cao, L., Yu, L., Gao, M., Ai, J., Gao, D., & Shang, Y. (2024). Deep learning-based characterization and redesign of major potato tuber storage protein. *Food Chemistry, 443*, Article 138556. https://doi.org/10.1016/j.foodchem.2024.138556

Nandakumar, A., Ito, Y., & Ueda, M. (2020). Solvent effects on the self-assembly of an amphiphilic polypeptide incorporating α-helical hydrophobic blocks. *Journal of the American Chemical Society, 142*(50), 20994–21003. https://doi.org/10.1021/jacs.0c03425

Neubauer, V. J., Trossmann, V. T., Jacobi, S., Döbl, A., & Scheibel, T. (2021). *Recombinant spider silk gels derived from aqueous–organic solvents as depots for drugs., 60*(21), 11847–11851. https://doi.org/10.1002/anie.202103147

Nikiforidis, C. V. (2019). Structure and functions of oleosomes (oil bodies). *Advances in Colloid and Interface Science, 274*, Article 102039. https://doi.org/10.1016/j.cis.2019.102039

Nikiforidis, C. V., Ampatzidis, C., Lalou, S., Scholten, E., Karapantsios, T. D., & Kiosseoglou, V. (2013). Purified oleosins at air–water interfaces. *Soft Matter, 9*(4), 1354–1363. https://doi.org/10.1039/C2SM27118D

Niu, Y., Li, Y., Qiao, Y., Li, F., Peng, D., Shen, W., & Huang, Q. (2024). In-situ grafting of dextran on oil body associated proteins at the oil–water interface through maillard glycosylation: Effect of dextran molecular weight. *Food Hydrocolloids, 146*, Article 109154. https://doi.org/10.1016/j.foodhyd.2023.109154

Pasaribu, B., Chen, C.-S., Liao, Y. K., Jiang, P.-L., & Tzen, J. T. C. (2017). Identification of caleosin and oleosin in oil bodies of pine pollen. *Plant Physiology and Biochemistry, 111*, 20–29. https://doi.org/10.1016/j.plaphy.2016.11.010

Peng, Y., Wang, C., Yu, J., Wu, J., Wang, F., Liu, Y., & Li, X. (2023). Self-assembly mechanism of rice glutelin amyloid fibril aggregates obtained through experimental and molecular dynamics simulation analysis. *Food Hydrocolloids, 143*, Article 108867. https://doi.org/10.1016/j.foodhyd.2023.108867

Plankensteiner, L., Hennebelle, M., Vincken, J.-P., & Nikiforidis, C. V. (2024). Insights into the emulsification mechanism of the surfactant-like protein oleosin. *Journal of Colloid and Interface Science, 657*, 352–362. https://doi.org/10.1016/j.jcis.2023.11.165

Plankensteiner, L., Yang, J., Bitter, J. H., Vincken, J.-P., Hennebelle, M., & Nikiforidis, C. V. (2023). High yield extraction of oleosins, the proteins that plants developed to stabilize oil droplets. *Food Hydrocolloids, 137*, Article 108419. https://doi.org/10.1016/j.foodhyd.2022.108419

Sun, Y.-L., Montz, B. J., Selhorst, R., Tang, H.-Y., Zhu, J., Nevin, K. P., & Emrick, T. (2021). Solvent-induced assembly of microbial protein nanowires into superstructured bundles. *Biomacromolecules, 22*(3), 1305–1311. https://doi.org/10.1021/acs.biomac.0c01790

Vargo, K. B., Parthasarathy, R., & Hammer, D. A. (2012). Self-assembly of tunable protein suprastructures from recombinant oleosin. *Proceedings of the National Academy of Sciences of the United States of America, 109*(29), 11657–11662. http://www.jstor.org/stable/41685133.

Wu, M.-H., Lin, M.-C., Lee, C.-C., Yu, S.-M., Wang, A. H. J., & Ho, T.-H. D. (2019). Enhancement of laccase activity by pre-incubation with organic solvents. *Scientific Reports, 9*(1), 9754. https://doi.org/10.1038/s41598-019-45118-x

Yang, K., Peng, H., Wen, Y., & Li, N. (2010). Re-examination of characteristic FTIR spectrum of secondary layer in bilayer oleic acid-coated Fe_3O_4 nanoparticles. *Applied Surface Science, 256*(10), 3093–3097. https://doi.org/10.1016/j.apsusc.2009.11.079

Yu, Y., Wang, J., Shao, Q., Shi, J., & Zhu, W. (2016). The effects of organic solvents on the folding pathway and associated thermodynamics of proteins: A microscopic view. *Scientific Reports, 6*(1), 19500. https://doi.org/10.1038/srep19500

Zhang, F., Zhu, F., Chen, B., Su, E., Chen, Y., & Cao, F. (2022). Composition, bioactive substances, extraction technologies and the influences on characteristics of Camellia oleifera oil: A review. *Food Research International, 156*, Article 111159. https://doi.org/10.1016/j.foodres.2022.111159

Zhang, W., Xiong, T., Ye, F., Chen, J.-H., Chen, Y.-R., Cao, J.-J., & Zhang, Z.-B. (2023). The lineage-specific evolution of the oleosin family in Theaceae. *Gene, 868*, Article 147385. https://doi.org/10.1016/j.gene.2023.147385

Zhao, L., Chen, Y., Chen, Y., Kong, X., & Hua, Y. (2016). Effects of pH on protein components of extracted oil bodies from diverse plant seeds and endogenous protease-induced oleosin hydrolysis. *Food Chemistry, 200*, 125–133. https://doi.org/10.1016/j.foodchem.2016.01.034

Zhong, M., Sun, Y., Song, H., Wang, S., Qi, B., Li, X., & Li, Y. (2023). Ethanol as a switch to induce soybean lipophilic protein self-assembly and resveratrol delivery. *Food Chemistry: X, 18*, Article 100698. https://doi.org/10.1016/j.fochx.2023.100698

Zhou, L.-Z., Chen, F.-S., Hao, L.-H., Du, Y., & Liu, C. (2019). Peanut oil body composition and stability. *Journal of Food Science, 84*(10), 2812–2819. https://doi.org/10.1111/1750-3841.14801

Zhou, Z., Wang, D., Luo, D., Zhou, Z., Liu, W., Zeng, W., & Sun, Q. (2024). Non-covalent binding of chlorogenic acid to myofibrillar protein improved its bio-functionality properties and metabolic fate. *Food Chemistry, 440*, Article 138208. https://doi.org/10.1016/j.foodchem.2023.138208